JOURNAL OF THE KOREAN ASTRONOMICAL SOCIETY
28: 15 ~ 30, 1995

THE VELOCITY INHOMOGENEITY IN THE COMA CLUSTER OF GALAXIES

KIM, KWANG TAE
Department of Astronomy and Space Science,
Chungnam National University, Daejeon 305-764, Korea
(Received Feb. 2, 1995; Accepted Apr. 13, 1995)

ABSTRACT

A velocity inhomogeneity, which is defined as a regional preponderence of either radial or tangential orbits, is searched with a *new* technique for the Coma cluster of galaxies. It is found within $\sim 2h^{-1}$ Mpc from the cluster center that the Coma shows conspicuous inhomogeneities in velocity and that the inhomogeneities are *real* at a 99% level of confidence. Even in the central region ($7' - 30'$ from the center), zones that are dominated by radial and tangential orbits are distinguishable. Defining the cluster's 'equator' as the direction defined by the Coma-A1367 supercluster, tangential orbits dominate the 'polar' zones in the central region. Galaxies that are located in $30' - 100'$ also inhomogeneous in velocity in that the 'polar' zones are mostly radial while the rest is nearly homogeneous. These results indicate that the Coma galaxies are exceedingly more *radial* in orbit, implying that merging or infalls are either still going on or an earlier virialization is likely to have occurred preferentially near the 'equator'.

Incorporating the velocity inhomogeneity into mass estimators, the most appropriate mass is turned out to be $0.4\times10^{15}h^{-1}M_{\odot}$ ($R \leq 0.6h^{-1}$Mpc), and $1.0\times10^{15}h^{-1}M_{\odot}$ ($R \leq 2.1h^{-1}$Mpc). The corresponding mass to blue light ratio on the average is $\sim 300h$. These estimates are consistent with Merritt (1987) and Hughes (1989) and the M/L_B is seemed to favour the mass-follows-light models than the uniform spread of dark matter throughout the cluster.

Key Words : galaxies: clustering–galaxies: intergalactic medium

I. INTRODUCTION

The Coma cluster of galaxies is the best-known example of a nearby, rich, regular, B-type (binary), and BM II (Bautz and Morgan 1970) cluster and is believed to be a part of a much larger, unbounded supercluster which lies in direction of A1367 (*cf.* Chincarini and Rood 1976; Tifft and Gregory 1976). The cluster shape is obviously elongated even with a visual inspection and this has been clearly shown by former investigators in which the elongation is along a position angle of $65° - 80°$ with the ellipticity of $0.55 \leq \epsilon \leq 0.7$, and which is marginally dependent on the radial distance from the cluster center, as well as on the brightness of the sample (Abell 1977; Schipper and King 1978; Thompson and Gregory 1978; Strimpel and Binney 1979). The asphericity of the Coma further reflects itself even in the central regions with the X-ray surface distribution (Chanan and Abramopoulos 1984; Briel *et al.* 1991), and this provides with a firm evidence for the underlying potential being not spherical virtually on all scales. The actual size is accordingly a matter of controversy: the angular radius ranges 1.7° (Noonan 1971), and 2.9° (Abell 1977), to at least 6° (Zwicky 1957).

Dynamics under a conventional assumption of a spherical system is only limited to the central part and even so, due both to a lack of knowledge of the possible distribution of dark matter and to insufficient velocity information of individual galaxies, our understanding of the structure such as the mass and velocity distributions remain far from perfect. The total mass of the Coma cluster has been computed with the positional and kinematical data by various authors (Abell 1977; Strimpel and Binney 1979; Kent and Gunn 1982; The and White 1986; Merritt 1987; Hughes 1989), and these form a large consensus that the mass is likely to be $(1\sim3)\times10^{15}h^{-1}\ M_{\odot}$ within a few Mpc from

the cluster (The parameter h is the Hubble constant in units of 100 km s^{-1} Mpc^{-1}.), and dynamic models (Merritt 1987) favors a mass to blue light ratio within 1 Mpc of $M/L_B \sim 350h$ and X-ray data (Hughes 1989) seem to best fit to a constant M/L_B of $180 \sim 500h$ extending to $2.5h^{-1}$ Mpc. Even if the cluster mass is effectively proportional to the radius of the circle out to which one includes galaxies (Strimpel and Binney 1979), as expected if Coma can be represented by an isothermal gas, the mass distribution depends on the velocity anisotropy (Merritt 1987), hence without knowing the velocity distribution the mass estimates can hardly be improved.

The crux of all of this matter is contained in the following question: are galaxy orbits in Coma primarily isotropic or radial? N-body simulations of cluster formation generally predict a preponderance of radial orbits near the cluster edge (Peebles 1970; Gott 1975; White 1976). Radial orbits are also suggested near the center by Bears and Tonry (1986) and Tonry (1986) in which the combined number density profiles of a set of clusters with dominant central galaxies is a power-law. Kent and Gunn (1982), however, suggest that the galaxies at large radii in Coma have considerably more kinetic energy in the tangential direction than would be predicted by the simulations. Assuming that mass follows light, Pryor and Geller (1984) found that the large number of HI rich spirals at large distances from the Coma center effectively rule out models with appreciable velocity anisotropies inside of approximately 7 times the core radius. On the other hand, Merritt (1987) points out that this inconsistency is a result of overly restrictive assumptions about the form of the velocity distribution function. Allowing sufficient flexibility in the choice of background potential and galaxy velocity distributions, he finds the following three general types of models to be consistent with the Coma velocity dispersion data: models in which the dark matter follows the galaxies, the galaxy velocities being roughly isotropic; models in which the dark matter is much more centrally concentrated than the galaxies, which have predominantly transverse velocities; and models in which the dark matter is spread nearly uniformly throughout the cluster, with the galaxy velocities being predominantly radial.

These results would be further complicated since the Coma on a large scale is not likely to be in statistical equilbrium and a spherical cluster is an obvious simplification in view of the apparent elongation and furthermore, the presence of subclusterings in Coma (Fitchett and Webster 1987) would significantly distort the velocity field. At this point, we might naturally ask if there is any other method least model dependent and directly probing the velocity structure. The answer is positive and here a *new* method is proposed which brings forth wealthy of information just we need.

The objective of this paper is to investigate the velocity structures of the Coma cluster and thereafter to re-estimate the mass of the system, employing the *new* technique suitable for finding velocity inhomogeneities (see § III) and using the redshift data which have significantly been increased in number over the last few years. The total number of redshifts within the velocity boundary of the Coma cluster includes previousely 280 samples (Kent and Gunn 1982). Adding 71 samples from the CfA survey (Huchra *et al.* 1990) and another 54 samples from Karachenstev and Kopylov (1990), the new data contain a total of 446 sample galaxies within about 6° radius circle (see § II for detail). The velocity inhomogeneity is studied for both the galaxies located near and far from the core region.

The organization of this paper is the following. In § II, the quality of the data is discussed briefly. The method diagonosing velocity inhomogeneities of the Coma is described in § III. The results are presented in § IV, and this is followed by the implications of the models and the mass estimates in § V. Discussion and conclusions are presented in § VI. Throughout this paper, the mean radial velocity of the Coma cluster is adopted to be 6932 km s^{-1} (Merritt 1987), which is essentially the same with the present data, and the angular conversion factor corresponds to $1' = 21h^{-1}$ kpc for the Coma.

II. THE DATA

The redshift data consist of those compiled in Kent and Gunn (1980; KG), the CfA survey (Huchra *et al.* 1990), and Karachenstev and Kopylov (1990; KK). This collection contains a total of 538 galaxy redshifts within a ~6° radius circular region from the cluster center. In the CGCG (the Catalogue of Galaxies and Clusters of Galaxies; Zwicky and Herzog 1963), there are a total of 365 galaxies brighter than 15.7 visual magnitude listed in the sample region of the sky. Among these, a total of 310 galaxies (85%) are listed in the present redshift data. Therefore, these samples are expected to represent the large scale velocity structure of Coma. The cluster center is adopted

Table 1. Magnitude Distribution.

Radius (1)	Magnitude (2)
0.0– 5.8	15.2±0.8
5.9– 10.1	15.2±0.8
10.2– 14.7	15.2±0.9
14.8– 19.9	15.2±0.6
20.0– 28.8	15.3±0.8
28.9– 42.9	15.4±0.8
43.0– 57.4	15.8±0.8
57.5– 73.4	16.0±1.0
73.5–101.2	16.0±0.9
101.3–129.0	15.6±0.7
129.1–195.8	15.6±0.9
195.9–245.0	15.4±0.9
245.1–276.7	15.4±0.9
276.8–455.2	15.1±0.7

Note: (1) Radius in minutes of arc; (2) Mean Zwicky Magnitude of the sample. The number of galaxies in each bin is 30.

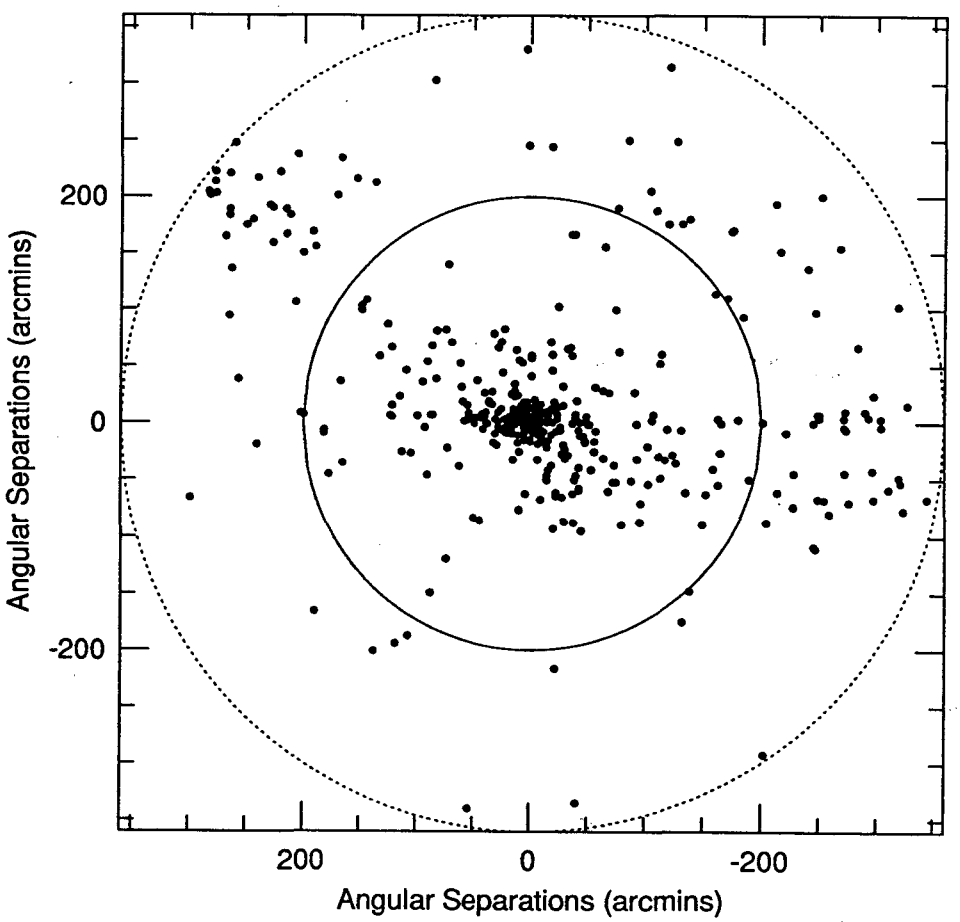

Fig. 1. Galaxies within the Coma velocity boundary $4000 \leq v_p \leq 10000\ km\ s^{-1}$ are plotted on a tangential plane (x-axis is in direction parallel to Right Ascension (1950.0)). The cluster center is at (x=y=0) $\alpha_c = 12^h\ 57^m\ 18^s$ $\delta_c = 28°\ 12'\ 48''$ (1950.0).Two circles are of $200'$ and $360'$ in radius. The galaxy group on the left top corner is the NGC 5056 group (Zwicky $160 - 7$) located at $13^h\ 20^m + 30.6°$.

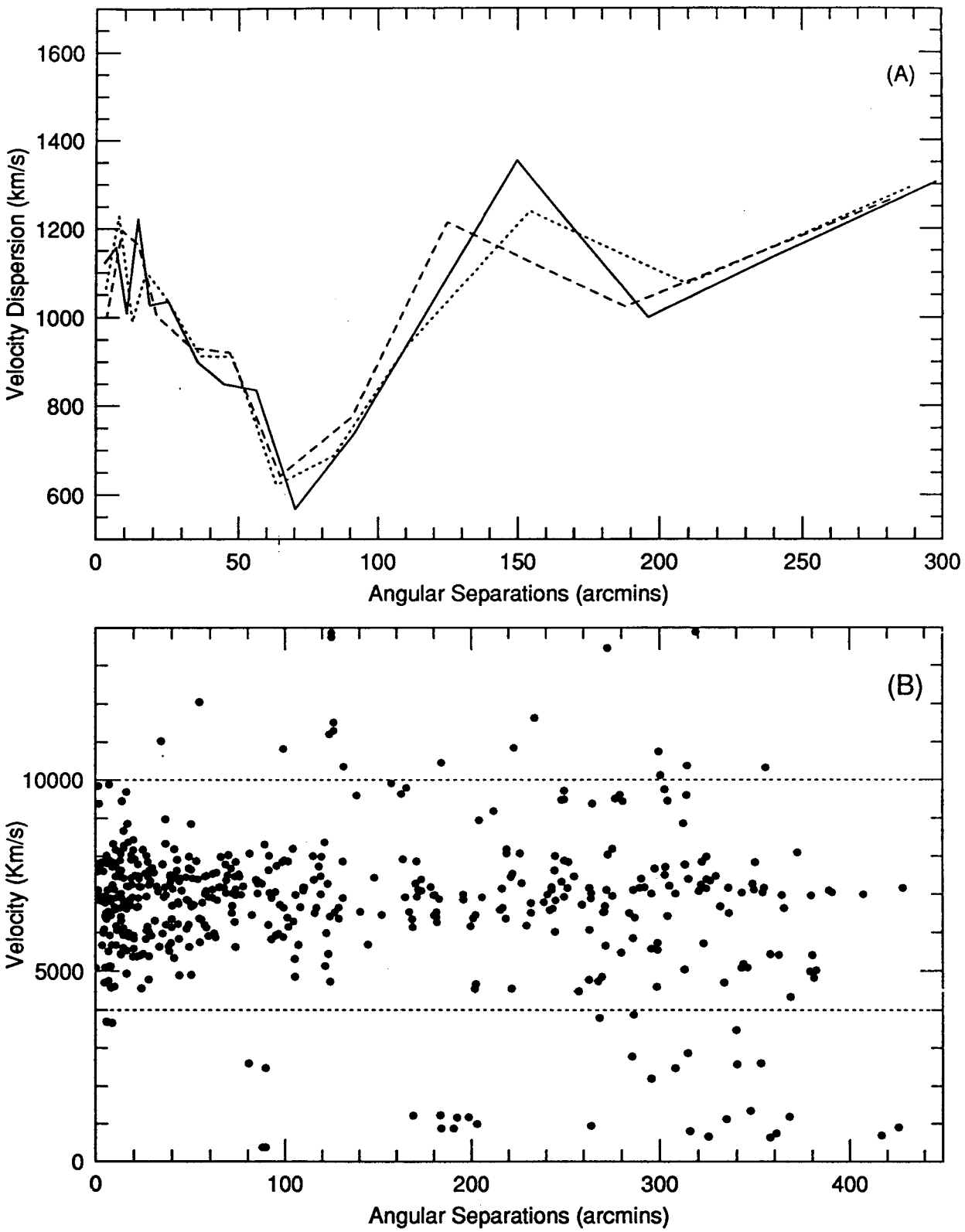

Fig. 2. In the upper panel (A) the velocity dispersions σ_p are shown with angular distances. Each bin contains 25, 30, 35 samples and these are drawn with solid, dot, and dash line, respectively. The whole samples are also shown in v_p with angular distances in the lower panel (B). The dotted lines are the velocity boundaries.

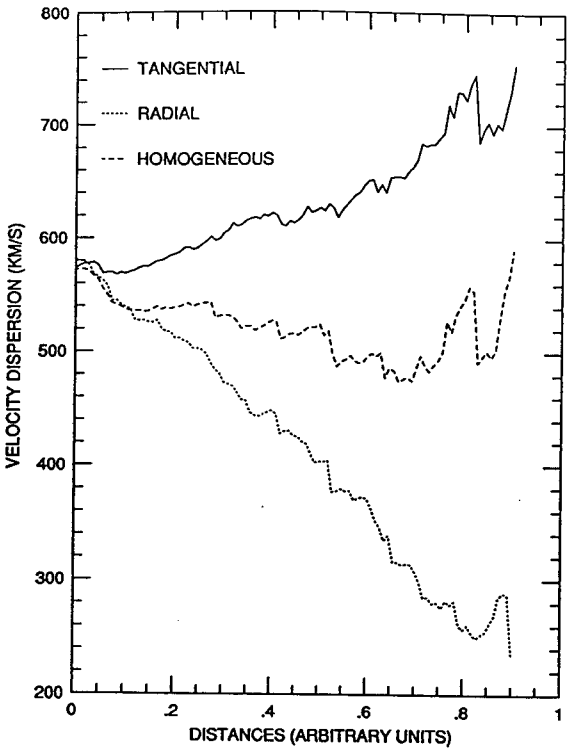

Fig. 3. This illustrates the variation of velocity dispersions with a size of central blockage for simulated systems. The 3-dimensional velocity dispersions of the simulations are 1000 $km\ s^{-1}$ and a total of 1000 particles are simulated for each set in which the density varies with r^{-2}. Three systems are simulated in that orbits are purely tangential (solid line), radial (dotted), and homogeneous (dash). The radial distances are in units of the system size. It is well shown, as described in the text, that tangential orbitors at larger distances increase σ_p, whereas the smaller σ_p is resulted when the more the radial orbitors were excluded near the center.

from Strimpel and Binney (1979): $\alpha_c = 12^h\ 57^m\ 18^s$, $\delta_c = 28^\circ\ 12'\ 48''$ (1950.0). The core radius is adopted to be $r_c = 8.5'$ (KG), and the galaxies whose radial velocity v_p are in the range of $4000 \leq v_p \leq 10000$ km s^{-1} are considered to be associated with the Coma cluster.

The data quality is examined in two points: distributions in magnitude and in mean radial velocity $< v_p(R) >$, both as a function of the projected radial distance R from the center. The former is to check if the sample is homogeneous in magnitude (hence in mass) and the latter to check both the large scale rotation and the velocity gradient in $< v_p(R) >$: if the velocity gradient is significant, this would give rise to an undesirable effect in $\sigma_p(R)$ as annular regions are conventionally taken for this. It turns out, however, that the magnitude distribution (blue) appears to be rather uniform and neither such gradient nor significant difference is noticiable in $< v_p(R) >$, especially even in the direction of the supercluster. The latter result is consistent with Rood *et al.* (1972) and Gregory (1975) who completely ruled out the rotation of the cluster as a whole. This assures that the present redshift sample is safe from the aformentioned effects.

In Table 1, the results are summarized, and the distributions of the samples in the tangential plane and in radial velocities are shown in Figs. 1, and 2.

It should be pointed out that the variation seen in $\sigma_p(\theta)$ (Fig. 2) is statistically very significant and the feature seen as a 'plateau', *i.e.*, beyond $\sim$100′ from the centre, is significantly broadened in velocity dispersion. It can be shown easily that an error in σ_p (i.e., the error in a standard deviation) is $\frac{\sigma_p}{2\sqrt{N}}$, where N being the number of a sample. Taking for example $N \approx 25$, this error becomes about 10% of the correponding velocity dispersion. On the other hand, the fluctuations expected due to the errors of the velocity data themselves, which are typically $100\sim200$ km s^{-1} (KG; KK and even smaller in the CfA survey), should be one order of magnitude smaller than $\frac{\sigma_p}{2\sqrt{N}}$, thus these may safely be ignored. To have a more formal ground for the statistical significance, nonparametric tests were applied. This result is summarized this way: comparing with the sample of minimum σ_p, those located

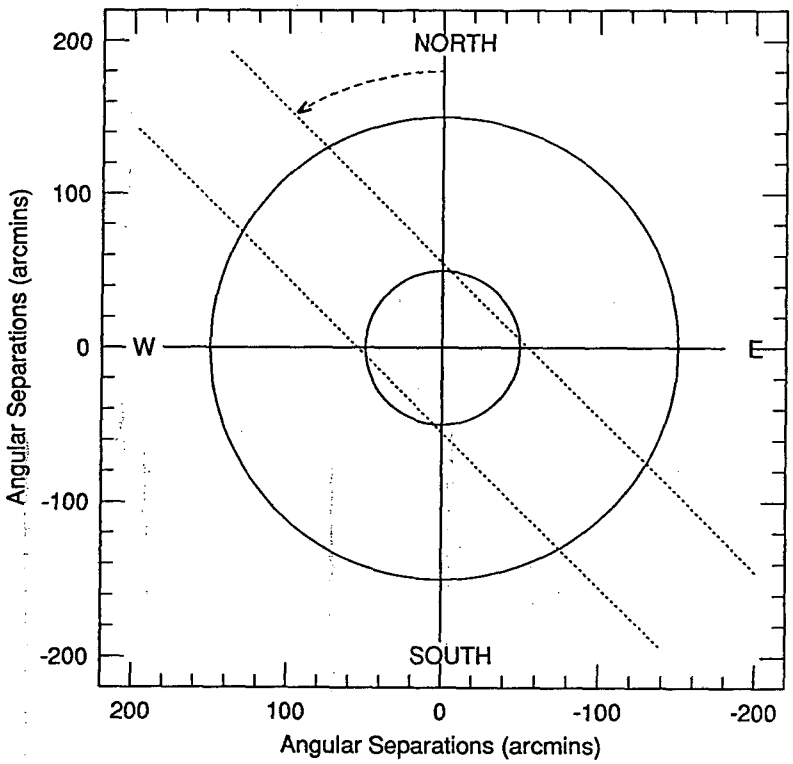

Fig. 4. This diagram illustrates the method measuring the inhomogeneity in the velocity dispersion. Centered on the cluster, two circles are drawn: the inner circle of r_i and outer circle of r_o in radius. Those galaxies that fall in the annular area are chosen for the test. A strip of a half width w is drawn at position angle χ and the velocity dispersion of the sample in the strip is calculated as χ is rotated from $0° - 180°$.

in $63' - 76'$, the core samples and those in the 'plateau' are both broadened in σ_p at a confidence level exceeding 99% (see § III.2 for the nonparametric tests).

III. THE METHOD DIAGNOSING VELOCITY INHOMOGENEITIES.

(a) Method

Even if the given set of velocity data suits our primary concern, examining the velocity inhomogeneity is not straightforward, In fact ambiguities arise due to the fact that we only have to deal with one dimensional data, the projected velocities v_p (KG; Merritt 1987). There is, however, one simple method bypassing the complications.

Suppose a spherical system consisting of bodies in various orbits, and consider it is seen at a certain line-of-sight. Radial orbitors that are seen projected near the center are clearly the main contributers to the overall velocity dispersion σ_p whereas those tangential orbitors there cause σ_p narrower. Excluding the central part from consideration, thusly supressing the effect of radial orbitors, these two groups of orbitors would significantly contrast in their contributions to σ_p. Now, consider a galaxy cluster and suppose velocity distribution is inhomogeneous in that orbits of galaxies in a certain direction in sky are mostly either tangential or radial. Excluding the central part and measuring σ_p for those galaxies located within a narrow strip, contrast will sure be enhanced when the position angle matches the direction of velocity inhomogeneity: the larger the central region is blocked, the sharper the contrast will be resulted. We illustrate this point in Fig. 3 with simulations.

This method requires no assumption and an application of this method is straightforward: a narrow stripe with a half width w and passing at a position angle χ through the cluster center is drawn, and the velocity dispersion is calculated for the subsample in the strip. The velocity inhomogeneity can be examined with $\sigma_p(\chi)$ by varying the position angle from 0 to 180 degrees. An illustration of this method is shown in Fig. 4. Tests of this method

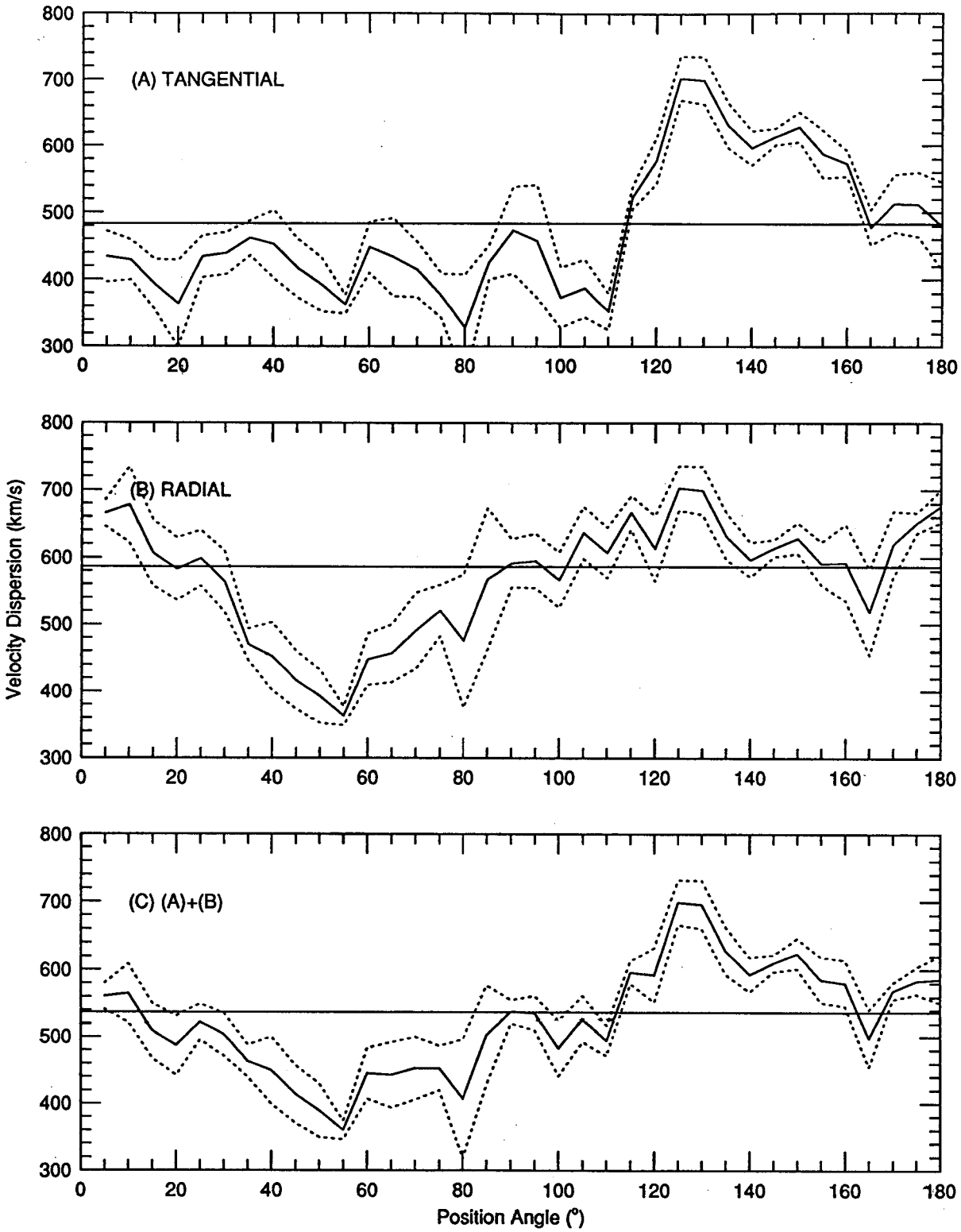

Fig. 5. The new method is applied to the simulated data to see how well this method recovers the input conditions. A static spherical system of 2000 particles following a r^{-2} density profile is simulated inside the system radius r_{sys}. Those particles contained in a strip of $w = 0.3r_{sys}$ at χ are assigned to have either radial or tangential as specified. In the first panel, the system is purely radial at $\chi = 50°$ and otherwise all are tangential; in the second panel, particles in $\chi = 140°$ are purely tangential and all in other regions are radial; these two sets of data are merged and this case is shown in the third panel. This clearly demonstrates the power of the method in recovering the input velocity inhomogeneity.

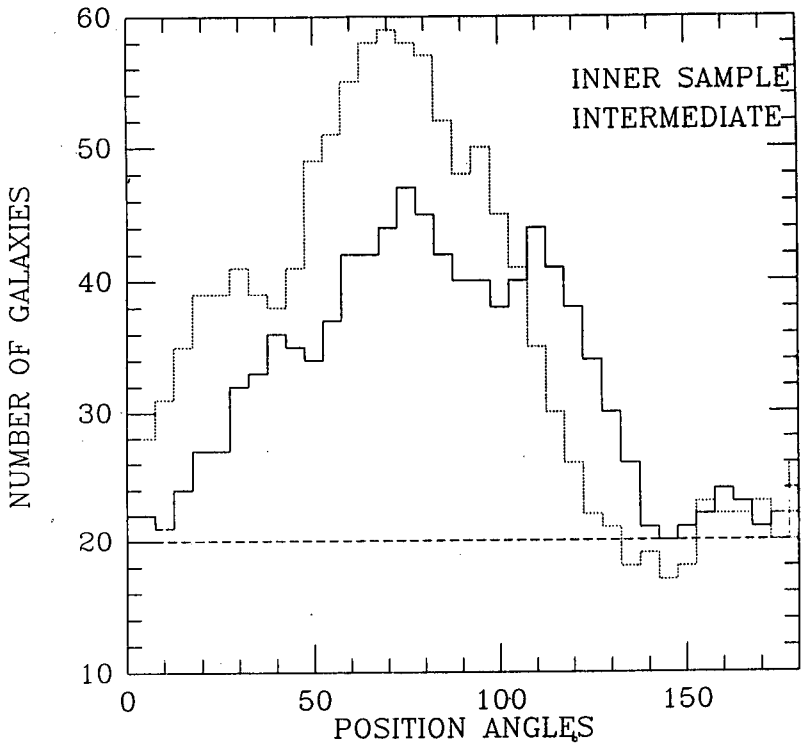

Fig. 6. The distributions of numbers of samples with χ are shown for the intermediate ($30' < \theta \leq 80'$) and the inner ($7' < \theta \leq 30'$) sample (inset). Both sample show strong spatial anisotropies: the Coma clearly elongates in direction of $\chi \approx 70°$. Sampling parameters were adjusted to keep the resulting statistics reliable for all different χ's: the minimum number of sample was taken to be about 20. Starting from the sample taken at $30' - 60'$, increments in number in each bin are shown for $r_0 = 80'$, $100'$ and $150'$.

are made with simulations and its superb ability in uncovering the velocity inhomogeneity is clearly demonstrated. The results of the tests are summarized in Fig. 5. There are three points noteworthy. Firstly, for real velocity data, the results are sensitively depends on the choices of w, the inner r_i, as well as on the outer radius r_o of the circles. One should adjust these parameters to match the underlying inhomogeneity, *i.e.*, to maximize the contrast while keeping the signal-to-noise ratio sufficiently large. Secondly, when the sample distribution in space is increasingly anisoptropic outward, one should keep r_o within the region where the anisotropy is not so severe; otherwise a fictitious inhomogeneity is likely to be resulted. Finally, inclusion of a wing component in the v_p distribution makes the resulting statistics unstable; inclusion of a few more galaxies causes the σ_p to change a lot, which is undesirable. To avoid this, the wing component is eliminated iteratively: Any galaxies whose v_p is more than $3\sigma_p$ different from the mean is eliminated and the mean and σ_p are recalculated with the remaining galaxies. This new σ_p is used to eliminated more samples and this iteration is continued until no further samples are eliminated.

(b) The Velocity Inhomogeneity and The Statistical Tests

It is certainly wise to investigate the velocity inhomogeneity not on a whole cluster scale but on a reasonable area where galaxy samples are well populated. Otherwise, one may lose possible fine structures that are smeared over a large scale. For the case of the Coma, the best application was made when the whole sample were divided into two classes: those galaxies located within $30'$ radius (the inner region) and the ones located in $30' - 80'$ (the intermediate region). These two samples are defined hereafter as the *inner* and the *intermediate* sample, respectively. Note that if galaxies further than $80'$ were included, samples begun to show their spatial anisotropy.

In Fig. 6, distributions of the samples in number are shown in histograms for the two regions. In Fig. 7, the $\sigma_p(\chi)$ are shown for the two samples. The best choices, trying various combinations of w, r_i, and r_o, are turned to be:

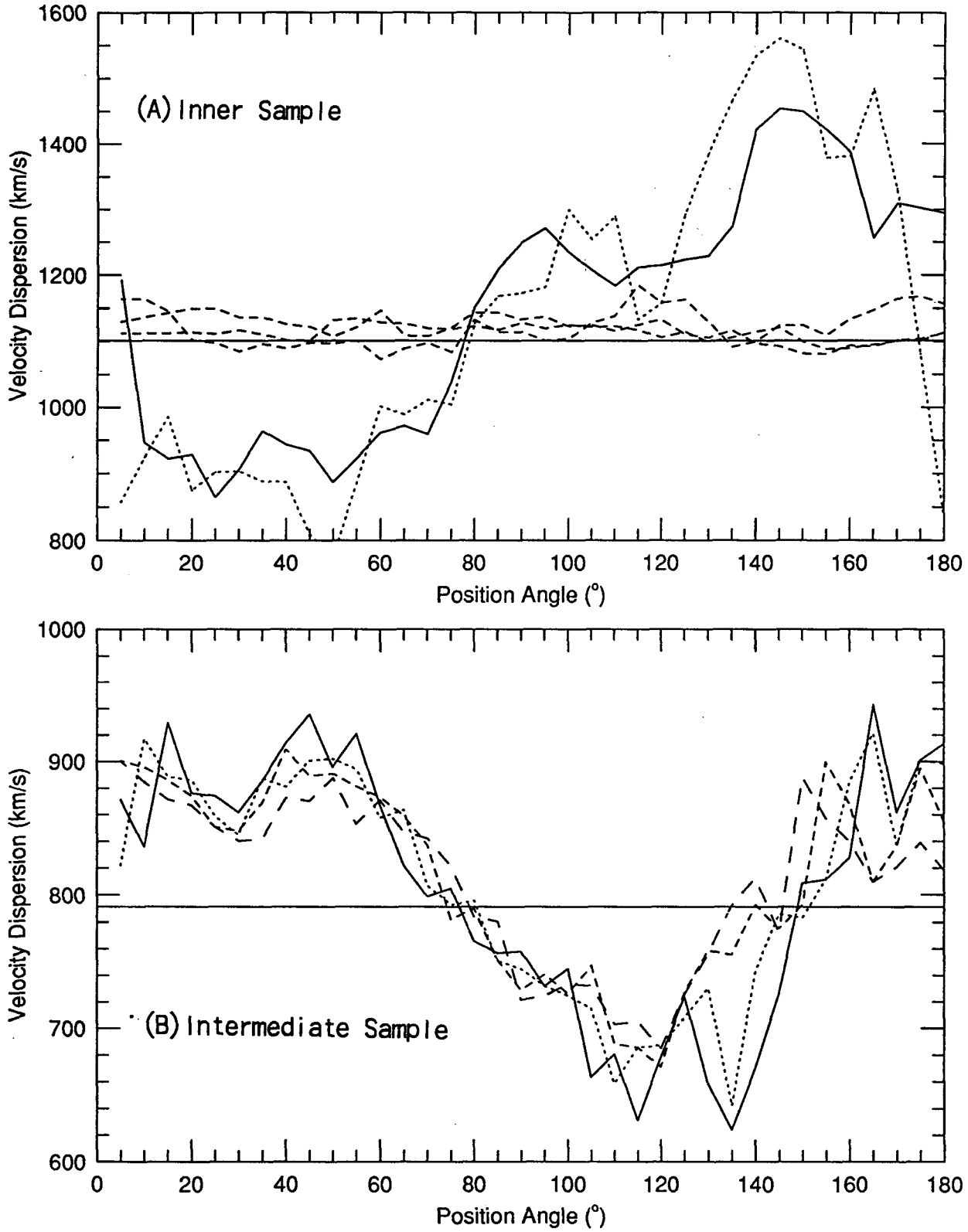

Fig. 7. The velocity inhomogeneities of the Coma cluster are shown for both the inner ($7' - 30'$; upper panel) and the intermediate sample ($30' - 100'$; lower panel). The number of samples in a strip is chosen to be larger than about 20 for reliable statistics (see Fig. 6). Different lines are due to different strip width: $w = 4'$ (dotted), $5'$ (solid), $6'$ (dashed) in the upper panel; $w = 24'$ (solid), $26'$ (dotted), $28'$ (dashed) in the lower panel. The solid straight lines represent the σ_p of the samples.

$w = 6'$, $r_i = 7'$, $r_o = 30'$ (inner sample),
$w = 28'$, $r_i = 30'$, $r_o = 80'$ (intermediate sample).

Apparently there exists variations in Fig. 7. That is a good sign. The question that bears all the essence of the method is if the variations in Fig. 7 are really *significant*? A simple estimate shows that the amplitudes of the variations are larger than two times the corresponding errors, which are $2\sigma_{\sigma(N)}$, implying $> 2\sigma$ level of confidence (>95%). But this is not enough, because samples in bins are not numerous enough that one cannot fully count on the Gaussian statistics. This substantiates further confirmations with some nonparametric tests. Here two nonparametric tests are applied: Ansari-Bradley (1960) and Kolmogorov-Smirnov two-sample test. The Ansari-Bradley test is a distribution-free rank sum test for *dispersion* which tests the hypothesis that the test population is broadened/narrowed. This test only involves the assumptions that the parent populations of both samples under comparison have the same median and that the distribution function governing the population in the absence of any velocity inhomogeneity is the same. The result is a test statistics W^*, which in the large sample approximation (Hollander and Wolfe 1973) is valid here. It can be treated as a σ value with the corresponding probability given by the tables for the normal distribution. For the Kolmogorov-Smirnov test, the one-tailed test is employed here which is used to find the probability of a match between the distribution arising from chance.

Comparing a sample taken at a χ with other samples at different χ's, and varying the χ from $0° - 180°$, the results of the two tests are arrays of W^* and the chance probabilities. We only choose the pairs of samples which distributions are likely to be drawn from different populations at a confidence level greater than 95%. These results are shown in Fig. 8 and the selected results of the statistical tests are summarized in Table 2.

Clearly enough, the nonparametric tests indicate that the variations in $\sigma_p(\chi)$ are *significant*. For example, the pairs defined by $\chi = 55°$, and $165°$ in the inner sample differ in dispersion at a confidence level greater than 99%. In the case of the intermediate sample, $\sigma_p(\chi)$ of the sample at $\chi \sim 95°$ is narrower than those at $\chi \sim 55°$, and $\sim 160°$ at confidence levels exceeding 99%, especially with the Kolmogorov-Smirnov test. These results therefore provide a formal ground that the velocity inhomogeneities are *real* at a 99% level of confidence.

IV. IMPLICATIONS AND MASS ESTIMATE

(a) Orbits and Alignment to the Supercluster

The velocity inhomogeneities seen in the Coma (Fig. 7) can now be interpreted straightforwardly in light of the simulations above. First, orbits of the galaxies in the inner region are obviously not homogeneous in distribution: tangential orbits are predominant at $\chi \sim 160°$ (the Hump) and the other region (the Dip I) is dominated by radial orbitors. When an annular average is taken in the inner region, this inhomogeneity is smeared out and thus one might easily oversight the inhomogeneity.

Secondly, galaxies in the intermediate regions are exceedingly more *tangential*: the preponderence of radial orbits is indicated by the feature at $\chi \sim 95°$ (the Dip II) and the orbits in the rest of the region are more tangential. If a cluster 'equator' is defined by the direction defined by Coma-A1367 supercluster, which is $\chi \sim 57°$, the 'equator' is well included in the Dip I and this is nearly perpendicular to the direction of the Hump and the Dip II. Intriguing is that the orbital preponderence of the galaxies in the 'polar' zones changes dramatically from *radial* to *tangential* inwardly from the intermediate 'polar' zones. This feature fits naturally into the infall picture in that galaxies which started infalls with radial orbits afar would naturally experience changes to tangential orbits near the cluster center as their initial angular momenta were kept more or less constant. Since changes in the velocity distribution can only be realized by collisions between galaxies, this feature implies that the galaxy density (and the mass condensation if the dark matter follows light) in the central regions is not likely to be sufficiently high, otherwise the dynamic relaxation would soon virialize them to have their initial conditions quickly lost.

Contrastingly enough, the velocity distribution in the 'equatorial' directions is different: from *tangential* to *radial* inwardly. Since the number of galaxies is noticiably large and the large scale alignment develops in the same direction, any mechanism that demands a spherical symmetry such as the spherical infall cannot produce this structure. Instead, formations of large scale structures should have proceeded with an accompaniment of an earlier virialization via collapse toward the equator. This process would most naturally result in a homogeneous distribution

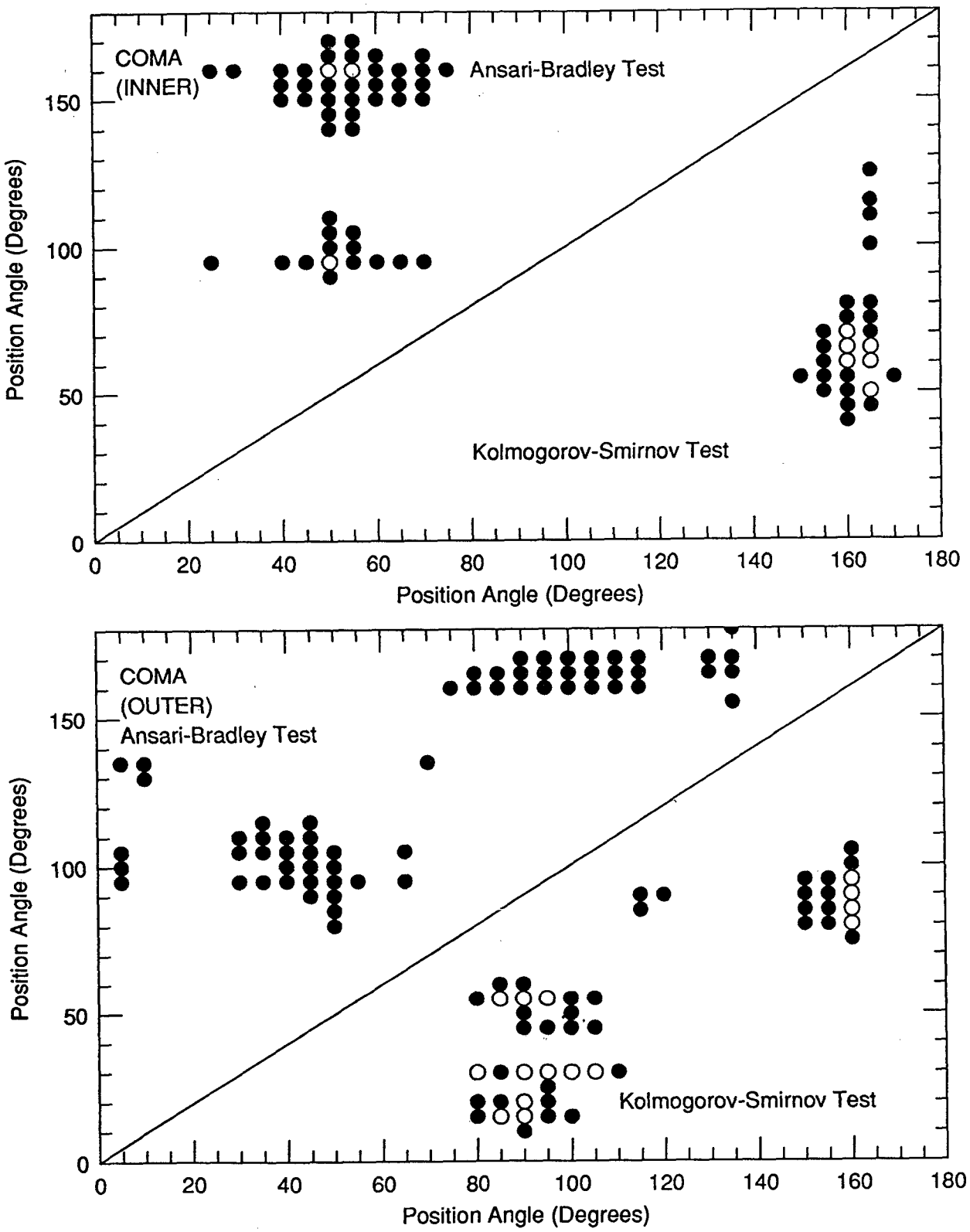

Fig. 8. Comparing the sample taken at a χ, with the other at different χ's and varying χ from $0° - 180°$, the results of the two nonparametric tests (Ansari-Bradley and Kolmogorov-Smirnov test) are the arrays of W^* and the chance probabilities, respectively. The pairs of samples which differ at a confidence level greater than 95 % are shown with filled circles: unfilled circles are the pairs which confidence levels exceed 99%.

Table 2. Selected Results of the Statistical Tests.

Sample (1)	χ_1 (2)	χ_2 (3)	N_1 (4)	N_2 (5)	$\sigma_p(\chi_1)$ (6)	$\sigma_p(\chi_2)$ (7)	W^* (8)	Confidence (9)
7−30	55	160	37	24	922.8	1387.4	+2.468	99.3
7−30	165	55	23	37	1256.7	922.8	KS	99.4
30−100	50	95	24	37	910.6	656.4	−2.202	98.6
30−100	95	160	37	10	656.4	902.3	+2.263	98.8
30−100	90	15	36	24	727.4	854.8	KS	99.3
30−100	90	55	36	32	727.4	890.3	KS	99.3
30−100	160	95	10	37	902.3	656.4	KS	99.2

Note: Column (1): Strip widths are $6'$ and $16'$ for the samples located within the regions defined by $(7' - 30')$ and $(30' - 100')$ radius from the centre. Column (2)-(3): Position angles in degrees. Two sub-samples are distinguished by subscripts. Column (4)-(5): Numbers of cluster galaxies in the strips. Column (6)-(7): Velocity dispersions in units of $km\ sec^{-1}$. Column (8): W^* is the test statistics of the Ansari-Bradley test (see text) and KS stands for the results of the Kolmogolov-Smirnov test. Column (9): Confidence levels in % ($|W^*| = 1.645$ and 2.330 correspond to 95% and 99% confidence level, respectively).

as is observed. Those galaxies in the equatorial directions subsequently felt more excess pull as they were nearer to the cluster center and this turned the orbits more to radial. The velocity structures inferred from Fig. 7 are summarized in Fig. 9.

(b) The Total Mass

Coma shows two definite signs for its not being in a dynamic equilibrium. First of all, $\sigma_p(R)$ is clearly the composite of two components: The inner part that can be described by King model and the 'halo' component which σ_p is more or less constant. Secondly, the velocity distribution is significantly inhomogeneous, even in the region near the core. Any mass estimates of Coma that are based on an equilbrium assumption would thus mislead. The prime concern is that which mass estimate would be most proper? This should be least model-dependent.

Incorporating the velocity inhomogeneity into conventional mass estimators (Heisler et al. 1985), the mass estimate would greatly be improved: in case when there are tangential orbits, the mass estimate is simple and the method is basically identical to the method proposed by Bahcall and Tremaine (1981). Suppose, there is a zone in which tangential orbits are predominant. Since the orbits are likely to be nearly circular, to which the virial theorem is readily applicable, the total mass within the orbits at R is given by

$$M(R) = \frac{\pi f_t < \sigma_p(R)^2 >}{2G < R^{-1} >} = \frac{f_t}{3} M_{\rm VT}, \quad (1)$$

where $M_{\rm VT}$ being the virial mass and f_t being the fraction of energy in the line-of-sight component of a tangential orbit: $\sigma^2 = f_t \sigma_p^2$ and obviously $1 \leq f_t < 3$. In case when the orbits are homogeneous, one half of the orbits are tangential, hence Eq. (1) is also applicable (and $f_t = 3$ is more appropriate). This argument is intuitively correct in the sense that the virial equilibrium is valid assumption for a self-gravitating system whose velocity distribution is homogeneous.

Applying Eq. (1) for the two samples, taking all the relevant values from § III, we estimate the total mass as

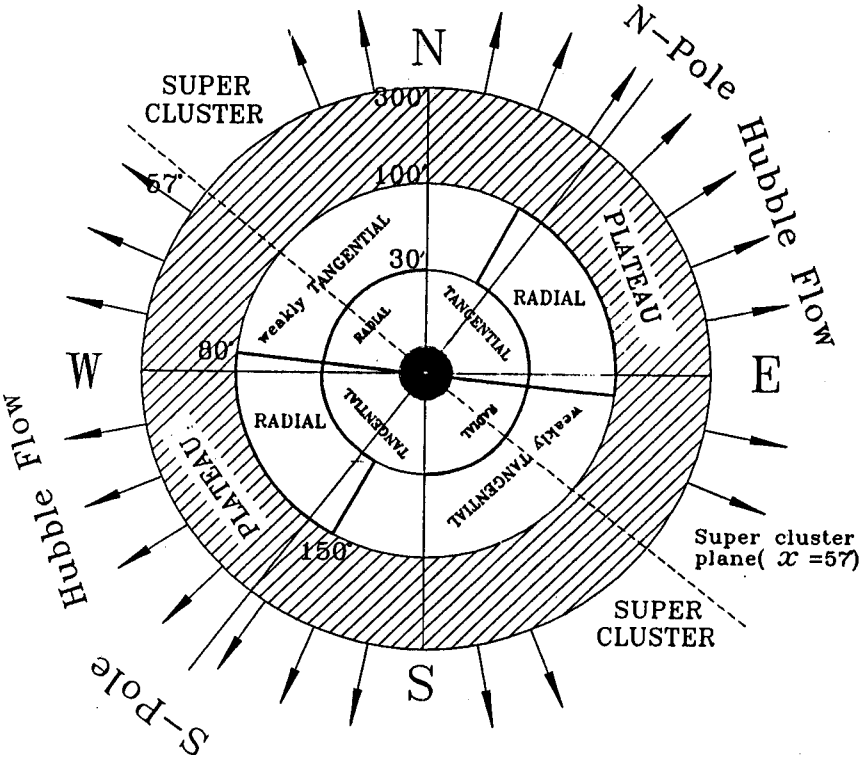

Fig. 9. This is a schemetic diagram summarizing the large scale velocity structure inferred from the test. The 'equator' lies in the direction of the Coma-A1367 supercluster and this direction is consistent, within error, with the direction derived from the galaxy distribtuion ($65^\circ - 80^\circ$). The orbits of the Coma galaxies as a whole are exceedingly *radial* and this supports the "infall" picture. The outermost circle represents the zero-velocity radius $R_{v=0}$, which is the cosmological radius where galaxies at this distance now turn from the Hubble flow into the cluster.

follows:

$$M(R) = \begin{cases} 0.4\times10^{15}h^{-1}\left(\frac{f_4}{2}\right)\left(\frac{<R^{-1}>^{-1}}{0.3\pm0.1\ \mathrm{Mpc}}\right)\left(\frac{\sigma_p}{1400\ \mathrm{km/s}}\right)^2 M_\odot & \text{if } R \le 0.6h^{-1}\mathrm{Mpc}; \\ 1.0\times10^{15}h^{-1}\left(\frac{f_4}{3}\right)\left(\frac{<R^{-1}>^{-1}}{1.1\pm0.4\ \mathrm{Mpc}}\right)\left(\frac{\sigma_p}{880\ \mathrm{km/s}}\right)^2 M_\odot & \text{if } R \le 2.1h^{-1}\mathrm{Mpc}. \end{cases} \quad (2)$$

As long as $\sigma_p(R)$ stays flat, the total mass obtained this way increases linearly with radius as previouely suggested by Strimpel and Binney (1979) and Hughes (1989).

The total luminosity is estimated with the cumulative luminosity function of the central regions by Godwin and Peach (1977; GP). Integrating the luminosity function, the total luminosity is simplified by $L = 4.33L^*N^*$, where N^* being the the total number of galaxies brighter than L^*, which is the luminosity of a galaxy at $m_v^* = 14.92$. The visual magnitude at the 'knee' of the luminosity function m_v^* is converted to $m_p^* = 15.86$ to Zwicky magnitude, via $m_p = m_v + 0.94$. Adopting the distance modulus of Coma to be 34.2 and the blue absolute magnitude of Sun as 5.48, I have $L^* = 3.4\times10^9h^{-2}L_\odot$ in blue light. Inside 30', what were found are 61 galaxies brighter than L^* in GP sample and inside 100', a total of 179 cluster members brighter than $m_p = 15.7$ are found in CGCG. Extrapolating to m_p^*, I estimate that $N^* = 227$. Thus the total blue light becomes $L_B = 0.89\times10^{12}h^{-2}L_\odot$ and $L_B = 3.3\times10^{12}h^{-2}L_\odot$ for the region inside 30' and 100' radius, respectively. These correspond to total mass to blue light radios as below: $M/L_B = (450\pm140)h$ ($R\le0.6h^{-1}$ Mpc), $M/L_B = (300\pm150)h$ ($R\le2.1h^{-1}$ Mpc) and consequently $M/L_B = (250\pm190)h$ for the region $0.6 < R\le2.1h^{-1}$ Mpc.

Considering the errors in the estimates, however, M/L_B is more likely to be constant with distance and this might favour the mass-follows-light model than the uniform spread of dark matter throughout the cluster. The former is consistent with the X-ray data (Hughes 1989) in that M/L_B lies in the range 280 to $380h$ $M_\odot/L_\odot$ for the regions within $2.5h^{-1}$ Mpc. A uniform distribution of the dark matter, on the other hand, should require M/L_B to increase with distance and this seems unlikely, unless the mass estimate was unrealistically underestimated least by a factor

of 2 to be consistent with the requirement.

V. DISCUSSION

The velocity distribution of a cluster is normally assumed to be a Gaussian. However, deviations from a Gaussain are often found in some clusters. Conventional interpretations invoke subclusterings and the presence of 'interlopers'. Additionally, the velocity inhomogeneity can in principle give a rise to a non-gaussian distribution. For example, suppose a cluster is dominated by tangential (radial) orbitors and, as is commonly the case, suppose the redshift data are limited to galaxies near the central regions. Then v_p distribution would be more (less) peaked at the mean than that expected from an homogeneous distribution. Thereafter, the velocity dispersion and consequently the mass of the cluster would then all be underestimated (overestimated). Inevitably, the error especailly in the mass estimate would obviously be substantial if the cluster has a significant inhomogeneity. The velocity inhomogeneity is of course very useful in estimating mass. Particularly the mass derived with tangential orbits would much improve the estimate. There is, however, a caution to be mentioned. Tangential orbits enhance σ_p of the zone and so one tends to have a larger mass using this information alone. To avoid this, f_t must be an adjusted properly in accordance to whether the system is tangential ($f_t \sim 3$) or homogeneous ($f_t < 3$). It is interesting to see how well this mass and the projected mass agree. Even if the system is dominated by radial orbits, one can use this method with the information of other zones: either homogeneous or tangential. Using the projected mass estimator with radial orbits (Heisler et al. 1985), which is $M = \frac{64}{\pi G} < R v_p^2 >$, the total projected masses are $(1.0 \pm 1.2) \times 10^{15} h^{-1} M_\odot$ (inside 30′), and $(1.7 \pm 2.0) \times 10^{15} h^{-1} M_\odot$ (inside 100′). As mentioned, Coma as a whole is dominantly radial, thus one expects the masses with the two different methods would agree and that is indeed so (except the large error). However, since the orbits near the core are only radial in part, an overestimation would be expected in the projected mass and in fact this is clearly about twice larger. Note that the projected mass for tangential orbits is exactly the half of it. This estimate is more consistent with ours, despite the orbits are not purely tangential, and this is primarily due to the fact that the relative contrast in σ_p of the tangential zone to the average is small (*i.e.*, $\sim \frac{1400}{1100} = 1.27$).

The degree of velocity inhomogeneity (which may be parameterized by the contrast in the $\sigma_p(\chi)$), and a cluster shape (or a X-ray isophotes), as well as the large scale structure of galaxies in relation to their orbital characters might be a good place to investigate for correlations. This may allow us to look more closely into the dynamic status and mass distribution of a galaxy cluster, possibly in relation to the early stage of cluster formation: *prolate* structures due to tidal fields (Binney and Silk 1979), *"pancake"* theories predict *oblate* structures (Sunyaev and Zel'dovich 1972), and dissipationless growth in anisotropies of the Hubble flow gives rise to all types of ellipsoids (Doroshkevich 1970). In the case of the Coma, its elongation in shape is consistent in direction with that inferred from tangential orbits. Recently, the dynamic nature of NGC 4839, based on the ROSAT X-ray observations (Briel *et al.* 1991), evidences for a merging event in the direction of $\chi = 41°$, which is again consistent with the predominance of radial orbits in roughly the same direction. Extending this type of diagnosis to other clusters, the power of this method is comfirmed and therein much useful information on their dynamic nature can be retrieved. For example, from Kim and Song (1995), two points are noteworthy: firstly, A2256 which is a Coma-like system, shows a very large inhomogeneity near the core regions and radial orbits also dominate in the direction of its elongation. This direction is clearly perpendicular to which tangential orbits are predominant and is also in good agreement with the position angle of measured with the X-ray surface brightness. Secondly, in case of the Hydra I cluster, the degree of inhomgeneity is found to be very small and this is just what we expected for a galaxy cluster like the Hydra whose X-ray distribution is almost circular. The velocity profile $\sigma_p(R)$ has an outstanding plateau developed from about 150′ and is seemed to persist to about 350′ from the center: the velocity data beyond this radius are too scanty to make any reasonable anaysis. Considering the preponderence of radial orbits and that the crossing times of the galaxies are comparable to the age of the Universe t_0, $\sigma_p(R)$ of the regions represents primarily the underlying mass distribution. A galaxy that just turned from Hubble flow into the cluster at the zero-velocity radius $R_{v=0}$ would increase its infall (radial) velocity with $(M(r)/r)^{\frac{1}{2}}$, thus the mass inside a radial distance $M(r)$ should increase linearly with radius r to be consistent with the plateau, suggesting that the mass density distribution in the regions is likely to follow an inverse square law. A high mass concentration to the cluster center can also be ruled out. The total mass, however, becomes infinity unless $M(r) \propto r$ breakes down beyond a certain boundary. This boundary is

estimated with the zero-velocity radius as given in Gunn and Gott (1972): $R_{v=0} = \left(\frac{8GMt_0^2}{\pi^2}\right)^{\frac{1}{3}}$, where M being the total mass of the Coma. Allowing $M(r) \propto r$ and extrapolating the mass, the total mass inside about 400′ becomes about the double of the mass given in Eq. (2), the resulting $R_{v=0}$ ranges from 5.2° to 7.7° ($6.5h^{-1}$ Mpc to $9.7h^{-1}$ Mpc), for q_0 varies from 1 to 0, respectively. This radius is well outside the plateau regions and we expect $\sigma_p(R)$ would fall off rapidly beyond $\sim R_{v=0}$. Interestingly enough, two point correlation studies indicate that the correlation length is in a good agreement with $R_{v=0}$: $7h^{-1}$ Mpc (Hewett 1982) and $9h^{-1}$ Mpc (Groth and Peebles 1977). More velocity data are substantiated for better understanding of the large scale structure of the Coma cluster of galaxies.

ACKNOWLEDGEMENTS

Author is appreciative to Dr. D. J. Song for helpful comments and discussion. This research was supported by the Korea Science and Engineering Foundation research grant 921-0200-010-1.

REFERENCES

Abell, G. O. 1977, ApJ, 213, 327
Ansari, A. R., and Bradley, R. A. 1960, Ann. Math. Stat., 31, 1174
Bahcall, J. N., and Tremaine, S. 1981, ApJ, 244, 805
Bautz, L. P., and Morgan, W. W. 1970, ApJL, 162, L149
Bears, T. C., and Tonry, J. L. 1986, ApJ, 300, 557
Binney, J. J., and Silk, J. 1979, MNRAS, 188, 273
Binney, J. J., and Strimpel, O., 1978, MNRAS, 185, 473
Briel, U. G. et al. 1991, A&A, 246, L10.
Chanan, G. A., and Abramopoulos, F. 1984, ApJ, 287, 89
Chincarini, G., and Rood, H. J. 1976, ApJ, 206, 30
Doroshkevich, A. G. 1970, Astrophysics, 6, 320
Fitchett, M. J., and Webster, R. 1987, ApJ, 317, 653
Geller, M. J., and Beers, T. C. 1982, PASP, 94, 421
Godwin, J. G., and Peach, J. V. 1977, MNRAS, 181, 323 (GP)
Gott, J. R. 1975, ApJ, 201, 296
Gregory, S. A. 1975, ApJ, 199, 1
Gregory, S. A., and Thompson, L. A. 1977, ApJ, 213, 345
Groth, E. J., and Peebles, P. J. E. 1977, ApJ, 217, 385
Gunn, J. E., and Gott, J. R. 1972, ApJ, 176, 1
Heisler, J., Tremaine, S., and Bahcall, J. N. 1985, ApJ, 298, 8
Hewett, P. C. 1982, MNRAS, 210, 867
Hollander, M., and Wolfe, D. A. 1973, Nonparametric Statistical Methods, (New York: John Wiley and Sons)
Huchra, J. P., Geller, M. J., de Lapparent, V., and Corwin, H. G. Jr. 1990, ApJS, 72, 433
Hughes, J. P. 1989, ApJ, 337, 21
Karachenstev and Kopylov 1990, MNRAS, 243, 390 (KK)
Kent, S. M., and Gunn, J. E. 1982, AJ, 87, 945 (KG)
Kim, K.-T., and Song, D. J. 1995, in preparation
Merritt, D. 1987, ApJ, 313, 121
Noonan, T. 1971, AJ, 76, 182
Peebles, P. J. E. 1970, AJ, 75, 113
Pryor, C., and Geller, M. J. 1984, ApJ, 278, 457
Rood, H. J., Page, T. L., Kintner, E. C., and King. I. R. 1972, ApJ, 175, 627
Schipper, L., and King, I. R. 1978, ApJ, 220, 798
Strimpel, O., and Binney, J. J. 1979, MNRAS, 188, 883
Sunyaev, R. A., and Zel'dovich, Ya. B. 1972, A&A, 20, 189

The, L. S., and White, S. D. M. 1986, AJ, 92, 1248
Tifft, W. G., and Gregory, S. A. 1976, ApJ, 205, 696
Thompson, L. A., and Gregory, S. A. 1978, ApJ, 220, 809
White, S. D. H. 1976, MNRAS, 177, 717
Zel'dovich, Ya. B., Einasto, J., and Shandarin, S. F. 1982, Nat, 300, 407
Zwicky, F., and Herzog, E. 1963, *Catalogue of Galaxies and Clusters of Galaxies*, Vol. **2**, pp. 314-319 (CGCG)